Throughput and delay analysis for IEEE 802.11 multi-hop networks considering data rate

Takeshi Kanematsu[1] (iD)**, Kosuke Sanada[2], Zhetao Li[3],
Tingrui Pei[3], Young-June Choi[4], Kien Nguyen[1]** (iD) **and Hiroo Sekiya[1]**

Abstract

In an IEEE 802.11 Distributed Coordination Function–based wireless network with multiple hops, a node operates on its own with several predefined data rates (i.e. following modulation and coding schemes). Moreover, the IEEE 802.11 Distributed Coordination Function node's communication is characterized by transmission and carrier-sensing distances. The transmission one is, in general, reverse proportional to the data rate. Meanwhile, the carrier distance keeps constant regardless of the modulation and coding scheme. Therefore, when a node has a high transmission rate, within its carrier-sensing range, the number of nodes may increase. The previous works have not yet extensively investigated the impact of data rates on such a scenario. This article addresses that issue aiming to quantify the network performance of the multi-hop IEEE 802.11 networks. As a solution, we propose the mathematical expressions, which consider data rates, for end-to-end throughputs, as well as delays in the network with string topology. We confirm the expressions' correctness by presenting the quantitative agreements between the analytical and simulation results.

Introduction

Recently, there has been renewed interest in adopting wireless multi-hop networks, which will be useful in various applications ranging from the traditional wireless sensor networks[1–3] to the Internet of Things[4–6] and vehicular ad hoc networks.[7–9] Such a system can relax the complexity of underlay infrastructure, hence improving the easiness and flexibility in network construction. More importantly, the wireless multi-hop networks enable the autonomous operations of network nodes, each of which is predetermined, for example, in a standard. This article focuses on the multi-hop networks in which each node's operation relies on the IEEE 802.11 Distributed Coordination Function (DCF). The IEEE 802.11 DCF defines the behaviors of medium access control (MAC) and physical (PHY) layers of a wireless node. Moreover, the physical data rates depend on predefined modulation and coding schemes.

[1]Chiba University, Chiba, Japan
[2]Mie University, Tsu, Japan
[3]Xiangtan University, Xiangtan, China
[4]Ajou University, Suwon, South Korea

Corresponding authors:
Kien Nguyen, Chiba University, Chiba 263-8522, Japan.
Email: nguyen@chiba-u.jp

Hiroo Sekiya, Chiba University, Chiba 263-8522, Japan.
Email: sekiya@faculty.chiba-u.jp

The operation of an IEEE 802.11 DCF node is following Carrier Sense Multiple Access/Collision Avoidance (CSMA/CA); hence, the transmission and carrier-sensing ranges are essential. In general, the one-hop transmission distance is inversely proportional to the data rate in the IEEE 802.11 standards. As a result, in a complete transmission within an identical end-to-end distance (ED), the number of nodes increases when the data rate increases, and vice versa. That results in the inherent trade-off between transmission speed and transmission distance when selecting the data rate. However, the node's carrier-sensing range is identical under the same transmission power. Therefore, the higher the data rate is, the more nodes exist in the carrier-sensing range, wherein the impact of frame collisions is not negligible. Motivated by that, this work aims to establish mathematical models considering the data rates accounting the issue.

In theory, several articles theoretically analyze the network performance of multi-hop wireless, mostly the string topology, using the airtime concept.[10–20] First introduced in Chung and Liew[10] for saturation throughput in IEEE 802.11 networks, the concept combines a contention graph to derive the saturated throughput model for a given source–destination pair in Gao et al.[11] In Sugimoto et al.,[13] the authors have extended the model to account for the throughput of two-way flows (of a VoIP traffic). Other IEEE 802.11 features such as Request To Send/Clear To Send (RTS/CTS), hidden node collision, long-frame communications, and back-off-stage synchronization have been investigated in previous studies,[14–16] respectively. In Qinjuan et al.,[17] the integration of airtime Markov chain analysis has well handled the IEEE 802.11 multi-hop network's unsaturated condition. The proposed model in Shimoyamada et al.[18] can formulate multi-hop networks' performance using the IEEE 802.11e Enhanced Distributed Channel Access (EDCA). In Sanada et al.,[19] the authors successfully derive the models that can manipulate varying hop number, frame length, and offered load. Besides the throughput, the airtime concept is also applicable for the delay analysis in multi-hop networks as in Sanada et al.[20] The previous works, however, often assume the carrier-sensing range is as twice as the transmission one. Hence, they have considered the varying number of nodes within a carrier-sensing range. As a result, the previous models cannot formulate the aforementioned trade-off caused by the data rates.

This article introduces the new theoretical analysis, which derives expressions for end-to-end throughputs and delays for IEEE 802.11 multi-hop networks. The expressions, which are formed from the airtime concept, efficiently assess the data rate parameter. The proposed model newly introduces the parameter η, which is the ratio of the carrier-sensing distance to the transmission one, to support any data rate. Another novelty is quantifying the duplication time of frame transmissions caused by the concurrent transmission, which often occurs at a high data rate. We have validated the proposed models by comparing the analytical results to simulation ones. The comparative results show that both results are well conformed.

The remainder of this article is organized as follows. Section "Background and related works" describes the related works about conventional models for multi-hop networks. Our analytical approach, which considers data rates, is presented in section "Proposed analytical models." In section "Evaluation results," we validate the proposed model by comparing its results to the simulation ones and discuss the network performance. Finally, we draw the conclusion for this work in section "Conclusion."

Background and related works

IEEE 802.11 data rates

There are multiple data rates (i.e. transmission speeds) in the physical layer of the IEEE 802.11 standards. Each defined data rate follows a modulation and coding scheme (MCS) index that includes a modulation type, a coding rate, several spatial streams, and an operation band. When the data rate increases, the signal of associated MCS becomes more sensitive to noise. Hence, the higher the data rate, the shorter the transmission distance in general. In a multi-hop IEEE 802.11 network, considering one-hop transmission, there is a similar trade-off between the transmission speed and the transmission distance. However, in such a scenario, the carrier-sensing range of a node is independent of the transmission speed. When a node operates at a high data rate, the number of nodes within its carrier-sensing range is more significant than that in a lower data rate operation. Therefore, to comprehend the trade-off within the carrier-sensing range of a node, it is necessary to consider the impact of hidden node and concurrent frame transmissions among the nodes.

Airtime concept

The airtime concept is a useful theory to understand the behaviors of the IEEE 802.11 wireless networks. During a duration, the theory can be used to characterize each IEEE 802.11 node's state corresponding to the IEEE 802.11 operation. More specifically, the IEEE 802.11 node is always in a transmission state, a carrier-sensing state, or an idle state. The first one indicates that the nodes' frames are being transmitted. The second one represents the condition in which the node detects frame transmissions of other nearby nodes. The last state means there is no transmission in the network. All the three states could be formulated in

consideration of the neighboring nodes' states. Hence, the airtime analysis is possible to express each network node's operation and the mutual effects between the nodes, and that is effective in the context of the multi-hop IEEE 802.11 network. The fundamental of airtime concept can be represented via the transmission airtime as follows. At Node i, the transmission airtime is defined as

$$X_i = \lim_{Time \to \infty} \frac{s_i}{Time} \qquad (1)$$

where s_i is the sum of several periods taken by frame transmissions from Node i to Node $(i + 1)$ in *Time* duration. More specifically, the periods include the durations of Distributed Inter-Frame Space (*DIFS*), a DATA frame transmission (*DATA*), Short Inter-Frame Space (*SIFS*), and an ACKnowledgement frame (*ACK*) transmission of Node i. The carrier-sensing and the idle airtime models can be accordingly derived following the network scenarios and other conditions.

Airtime-based analysis

The theoretical analysis using airtime concept has shown the applicability in IEEE 802.11 wireless networks under various conditions.[10–20] The airtime concept was initially proposed in Chung and Liew[10] to construct a model for the maximum saturation throughput. However, the model assumed that simultaneous frame transmissions are negligible. Moreover, it considers only collisions with hidden nodes for the sake of simplicity. The authors in Gao et al.[11] proposed the analytical model that combines airtime and contention graph to derive the throughput of a given source and destination pair. In Inaba et al.[12] and Sugimoto et al.,[13] the authors additionally considered two-way flows and RTS/CTS handshake, respectively. Both works have got the maximum throughput in multi-hop wireless networks. The proposed model in Zhao et al.[14] can analyze the intra-flow contention problem by expressing hidden node operation using airtime. In Sekiya et al.,[15] the applicable range of the airtime model has been extended from short-frame communication to long-frame communication. In Sanada et al.,[16] the mechanism of back-off-stage synchronization, which is efficient in multi-hop networks, was revealed. In Qinjuan et al.,[17] the authors proposed the bandwidth mapping model in unsaturated conditions by combining the airtime concept and the Markov chain model. The work in Shimoyamada et al.[18] established the mathematical model for multi-hop networks considering IEEE 802.11e EDCA. The generalized analytical model for string-topology multi-hop networks, which is applicable under any conditions of hop number, frame length, and offered load, has been proposed in Sanada et al.[19] The same authors have proposed the analytical models

for the end-to-end delay in multi-hop IEEE 801.11 networks in Sanada et al.[20] However, all these previous works assume a small number of network nodes in the carrier-sensing range, and that is because the carrier-sensing distance is assumingly the same or twice as the transmission distance. Therefore, all of them have not considered the condition where many nodes coexist in the same range. One of the recent works, which uses airtime concept, addresses the dense nodes but within a transmission range (i.e. single-hop), focusing on the capture effect.[21] In Liu et al.,[22] the airtime-based analysis has been also applied in dense wireless networks aiming to quantify the inter-network interference. The earlier results of this work have been presented at IEEE VTC Spring 2019.[23] In this article, we newly include the delay analysis, besides the throughput one. Moreover, the evaluation results are more extensive.

Proposed analytical models

This analysis expresses the difference in transmission distances that depends on the data rate using the ratio of the carrier-sensing distance to the transmission distance. We aim to derive the end-to-end throughput and delay as functions that take the ratio into account when modeling each network node's operation. Moreover, the airtime concept is used to quantify relationships among network nodes. Figure 1 shows the investigated network, which is an *H*-hop string-topology IEEE 802.11 one. In such a network, the wireless nodes are located at an identical distance, while the total distance from the source to the destination node is denoted as *ED*. The following analysis is based on several assumptions:

1. Node 0 is the only data source, which generates traffic to Node *H* (i.e. the destination). The traffic including fixed sized data frames follows the Poisson distribution.
2. The intermediate node (e.g. Node i) only relays the frame from Node $(i - 1)$ to Node $(i + 1)$.
3. All links have ideal channel conditions. In other words, the transmission failures occur only due to the MAC layer.
4. Node i can sense frame transmissions from Node $(i - \eta)$ to Node $(i + \eta)$, and that means Node $(i + \eta + 1)$ is the hidden node of Node i.

Transmission airtime

The transmission airtime, which is defined as the time-share of frame transmissions, includes both the successful and failure transmission durations.[10] Using the general expression of the transmission airtime in equation (1), the throughput of Node i can be expressed as
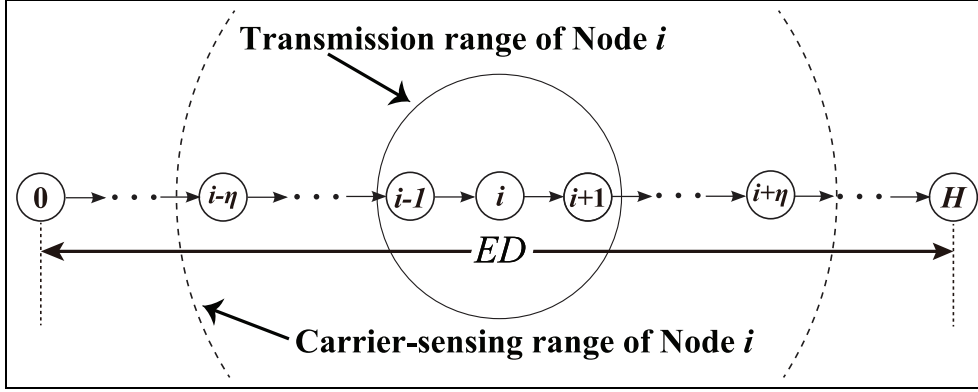
$$E_i = X_i(1 - \gamma_i)\frac{P}{T} \qquad (2)$$

Figure 1. Investigated wireless network topology with *H* hops and the end-to-end distance *ED*.

where γ_i is the collision probability of Node *i*; *P* is the payload size of data frame; and $T = DIFS + DATA + SIFS + ACK$.

Carrier-sensing airtime

The carrier-sensing airtime is known as the timeshare of the frame transmissions of the nodes in the carrier-sensing range. Considering the duplication time of frame transmissions, the carrier-sensing airtime of Node *i* is

$$Y_i = \sum_{\substack{j=i-\eta \\ j\neq i}}^{i+\eta} (X_j - D_{j,i}) \qquad (3)$$

where $D_{j,i}$ is the duplication time of Node *j* to be considered when calculating the carrier-sensing airtime of Node *i*. Duplications of transmission time are caused by concurrent frame transmissions or hidden node frame transmissions. In the previous works, the case of $\eta = 2$ is often assumed. When η is small, the main cause of the duplication is hidden node frame transmissions, and the duplication time caused by concurrent frame transmissions has been ignored in the conventional models. Our model, however, newly considers the duplication time due to concurrent transmissions to make it adaptable for the situation where many network nodes exist in the carrier-sensing range. Therefore, $D_{j,i}$ is expressed as

$$D_{j,i} = X_j \left(1 - \prod_{\substack{k\in\mu(j,i) \\ k>j}} (1 - \gamma_{k,j})\right)$$
$$+ \sum_{l=j+\eta+1}^{i+\eta} \frac{X_j \cdot X_l}{1 - \sum_{m\in\mu(j,l)} X_m \prod_{\substack{n\in\mu(j,l) \\ n>m}} (1 - \gamma_{n,m})} \qquad (4)$$

where $\gamma_{i,j}$ is the probability that Node *i* and Node *j* concurrently start transmitting a frame. The concrete expression of $\gamma_{i,j}$ is later described in section "Transmission probability." $\mu(i,j) = \psi(i) \cap \psi(j)$, where $\psi(i)$ is a set of nodes in the carrier-sensing range of Node *i*. In equation (4), the first term of the right-hand side means the duplication time due to concurrent frame transmissions, which is expressed using $\gamma_{i,j}$.

Channel-idle airtime

The channel-idle airtime is the timeshare that no neighbor node transmits a frame, and that means the node associated with the channel is not in either the transmission state or the carrier-sensing state. Therefore, the idle airtime is

$$Z_i = 1 - X_i - Y_i \qquad (5)$$

Collision probability

In the investigated topology, the frame collisions occur due to either the concurrent frame transmissions or the hidden node frame ones. Those collision events are, however, independent. Therefore, at Node *i*, the probability of frame collision is

$$\gamma_i = \gamma_{C_i} + \gamma_{H_i} \qquad (6)$$

where γ_{C_i} is the probability of concurrent-transmission collision, and γ_{H_i} is the one of the hidden node collisions.

The concurrent transmissions occur at Node *i* when at least one node within its carrier-sensing range transmits a frame at the same moment as Node *i* begins a fame transmission. Hence, the concurrent-transmission collision probability of Node *i* is

$$\gamma_{C_i} = 1 - \prod_{\substack{j=i-\eta+1 \\ j\neq i}}^{i+\eta} (1 - \gamma_{j,i}) \qquad (7)$$

From the assumption 4, we know that the hidden node of Node i is Node $(i + \eta + 1)$. The hidden node collisions of Node i occur when Node i starts transmitting a frame while Node $(i + \eta + 1)$ is transmitting or when Node $(i + \eta + 1)$ starts transmitting a frame while Node i is transmitting. Because these two types of collision happen independently, Node i's hidden node collision probability is expressed as

$$\gamma_{H_i} = \gamma_{H_i}^{(1)} + \gamma_{H_i}^{(2)} \qquad (8)$$

where $\gamma_{H_i}^{(1)}$ and $\gamma_{H_i}^{(2)}$ are the hidden node collision probabilities of the former type and the latter one, respectively.

The collision probabilities can be formed from a Markov chain model as in Figure 2.[19] In the model, d is the number of slots required for a DATA frame transmission; W_s is the contention window at back-off stage s. W_s is calculated as

$$W_s = \begin{cases} 2^s(CW_{min} + 1) - 1 & 0 \le s \le L' - 1 \\ CW_{max} & L' \le s \le L \end{cases} \qquad (9)$$

where CW_{min} and CW_{max} are the minimum and maximum values of contention window, respectively. L is the maximum back-off stage and $L' = \log_2 (CW_{max} + 1/CW_{min} + 1)$. S is the smallest number of back-off stages that satisfies $d \le W_s$. This Markov chain model includes the back-off timer (BT) decrement state and transmission state. In the two dimensional parameters $[s, t]$, where s means the back-off stage, and t means the BT in BT-decrement state and the number of elapsed slots in the transmission state. Using the model, the relationship among network nodes in the local time duration can be expressed.[19]

From the Markov chain model in Figure 2, $\gamma_{H_i}^{(1)}$ and $\gamma_{H_i}^{(2)}$ are expressed as

$$\gamma_{H_i}^{(1)} = \frac{\theta_{i+\eta+1}\alpha_{i+\eta+1}}{1 - \sum\limits_{j \in \mu(i+\eta+1,i)} X_j \prod\limits_{\substack{l \in \mu(i+\eta+1,i) \\ l > j}} (1 - \gamma_{l,j})} \qquad (10)$$

$$\gamma_{H_i}^{(2)} = \frac{\theta_{i+\eta+1}\beta_{i+\eta+1}\left(1 - \sum\limits_{k \in \nu(i+\eta+1,i)} X_k \prod\limits_{\substack{l \in \nu(i+\eta+1,i) \\ l > k}} (1 - \gamma_{l,k})\right)}{1 - \sum\limits_{j \in \mu(i+\eta+1,i)} X_j \prod\limits_{\substack{l \in \mu(i+\eta+1,i) \\ l > j}} (1 - \gamma_{l,j})} \qquad (11)$$

where $\nu(i + \eta + 1, i) = \psi(i + \eta + 1) \cap \overline{\psi(i)}$. θ_i means the timeshare that Node i belongs to the state represented by the Markov chain model. Hence, θ_i is expressed as

$$\theta_i = aX_i + q_iZ_i \qquad (12)$$

where $a = DATA/T$ and q_i is the frame-existence probability of Node i, which is described in detail in the next section. α_i and β_i are the sum of stationary distributions of Node i that belong to the transmission state and the state with $0 \le t \le d$ on the Markov chain model, respectively. Using the stationary distribution of Node i in the Markov chain model, $b[s, t]_i$, we have

$$\alpha_i = \sum_{s=0}^{L} \sum_{t=-d}^{-1} b[s, t]_i \qquad (13)$$

and

$$\beta_i = \sum_{s=0}^{S-1} \sum_{t=0}^{W_s} b[s, t]_i + \sum_{s=S}^{L} \sum_{t=0}^{d} b[s, t]_i \qquad (14)$$

Frame transmission probability

At Node i, the probability of frame transmission is the probability that the node starts frame transmission when being in the idle state. More specific, the node attempts to transmit a frame when its BT is zero. From the Markov chain model in Figure 2, the frame transmission probability of Node i in the saturated condition is

$$G_i = \frac{\sum\limits_{s=0}^{L} b[s, 0]_i}{\sum\limits_{s=0}^{L} \sum\limits_{t=0}^{W_s} b[s, t]_i} \qquad (15)$$

In the case of expressing the non-saturated condition, we need to define the frame-existence probability, q_i. q_i is the probability that Node i has at least one frame when Node i's state is idle. When a node has frames in the idle state, it decreases BT. Therefore, the airtime for BT decrements is

$$W_i = q_i'Z_i \qquad (16)$$

where q_i' is the frame-existence probability in the non-saturated condition. The expected spending time for BT decrement with one successful frame transmission is expressed as $V_i\sigma$, where σ is the system slot time. Besides, V_i, which is the expected slot number of BT decrement for one successful frame transmission, is expressed as

$$V_i = \sum_{s=0}^{L} \frac{\gamma_i^s(W_s + 1)}{2} \qquad (17)$$

Therefore, the airtime for the BT decrement is

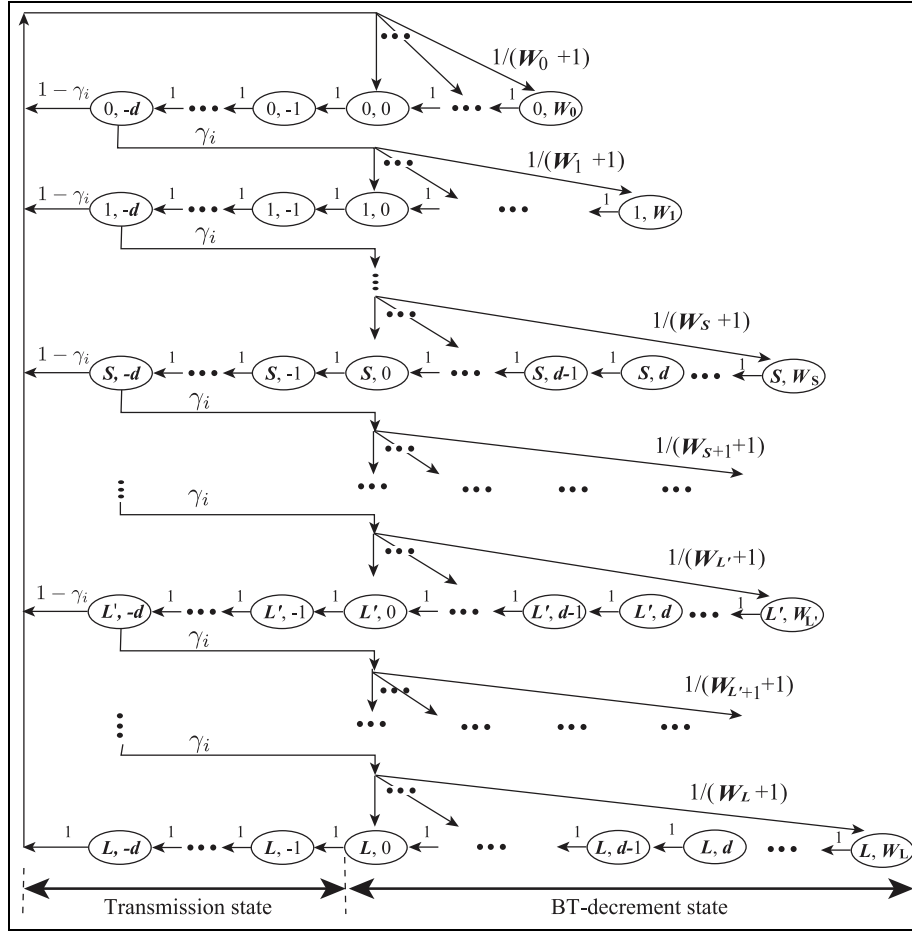$$W_i = \lambda_iV_i\sigma \qquad (18)$$

Figure 2. Node i's Markov chain model with the back-off timer decrement and transmission states in case of $S<L'$.

where λ_i is the frame reception rate of Node i, which can be expressed by the throughput of Node $(i-1)$ following the assumption 2 as follows

$$\lambda_i = \frac{E_{i-1}}{P} = \frac{X_{i-1}(1-\gamma_{i-1})}{T} \qquad (19)$$

In equation (19), E_{-1} is the offered load of the string-topology network. By equating right-hand side of equations (16) and (18), q_i' is obtained as

$$q_i' = \frac{\lambda_i V_i \sigma}{Z_i} \qquad (20)$$

We know that the frame-existence probability in the saturated condition is one. Therefore, the frame-existence probability in the whole time can be expressed as

$$q_i = \min(1, q_i') = \left(1, \frac{\lambda_i V_i \sigma}{Z_i}\right) \qquad (21)$$

Using the probability in equation (21), the frame transmission probability is

$$\tau_i = q_i G_i \qquad (22)$$

which is also valid for both the non-saturated and saturated states. Considering the number of frame transmissions per unit time and the time for one frame transmission success, the transmission airtime of Node i is expressed by

$$X_i = \frac{q_i G_i Z_i T}{\sigma} \qquad (23)$$

In addition, the probability that Node i and Node j simultaneously start transmitting a frame is expressed as

$$\gamma_{j,i} = \tau_j \omega_{j,i} \qquad (24)$$

where

$$\omega_{j,i} = 1 - \sum_{k \in \nu(j,i)} X_k \prod_{\substack{l \in \nu(j,i) \\ l > k}} \left(1 - \gamma_{l,k}\right) \qquad (25)$$

End-to-end throughput

In the string-topology network with H hop, the end-to-end throughput can be derived as

$$E = E_{H-1} \qquad (26)$$

End-to-end delay

The definition of end-to-end delay in this work is similar to the one in Sanada et al.[20] The delay is the duration from the moment that the DATA frame is generated at the source node to the instant when the destination node receives the DATA frame. In other words, the end-to-end delay is the sum of multiple delays of single-hop transmission from the source node to the destination node. However, the single-hop transmission delay includes two types of delays, which are the MAC access delay and the queueing one.

The frame-existence probability, q_i, is previously defined in the channel-idle state. In the carrier-sensing state, the probability is assumingly as same as the total time. Therefore, the frame-existence probability in the total time is expressed as

$$Q_i = X_i + q_i Z_i + Q_i Y_i \qquad (27)$$

From equation (27), we have

$$Q_i = \frac{X_i + q_i Z_i}{1 - Y_i} = \frac{X_i + q_i Z_i}{X_i + Z_i} \qquad (28)$$

Figure 3 shows the $M/M/1$ buffer queueing model of Node i in the multi-hop network. In the model, the service time is the duration from the instant that a frame reaches the top of node buffer to the instant that a frame transmission is successful. The service time consists of the durations of BT decrements, BT freezing, and frame transmissions. Therefore, the MAC access delay of Node i is

$$
\begin{aligned}
D_{M_i} &= T_i R_i \left(1 + \frac{Q_i Y_i + q_i Z_i}{X_i}\right) \\
&= T_i R_i \left[1 + \frac{X_i Y_i + q_i Y_i Z_i + q_i X_i Z_i + q_i Z_i^2}{X_i(X_i + Z_i)}\right] \\
&= T_i R_i \left[\frac{(X_i + q_i Z_i)(X_i + Y_i + Z_i)}{X_i(X_i + Z_i)}\right] \\
&= \frac{T_i R_i (X_i + q_i Z_i)}{X_i(X_i + Z_i)}
\end{aligned}
\qquad (29)
$$

The queueing delay is the time duration from the instant that Node i receives a frame to the instant that the frame reaches to the top of Node i's buffer. Using
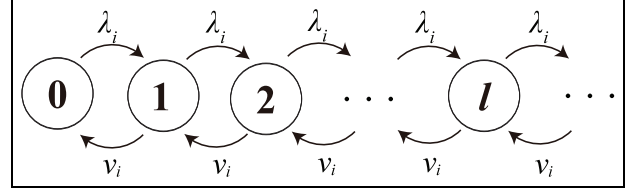

Figure 3. Node i's buffer queueing model.

the service time in equation (29), the service rate of the model in Figure 3 can be as follows

$$v_i = \frac{1}{D_{M_i}} = \frac{X_i(X_i + Z_i)}{T_i R_i(X_i + q_i Z_i)} \qquad (30)$$

Since we know the frame reception rate from equation (19) and the service rate from equation (30), the buffer utilization rate of Node i can be derived in equation (31)

$$\rho_i = \frac{\lambda_i}{v_i} = \frac{\lambda_i T_i R_i(X_i + q_i Z_i)}{X_i(X_i + Z_i)} = \frac{X_i + q_i Z_i}{X_i + Z_i} = Q_i \qquad (31)$$

From the model in Figure 3, we can derive the steady-state probability that the Node i has l frames as

$$b_{i,j} = \frac{\lambda_i}{v_i} b_{i,l} = \cdots = \left(\frac{\lambda_i}{v_i}\right)^i b_{i,0} = Q_i^l b_{i,0} \qquad (32)$$

Because $b_{i,0}$ is the steady-state probability in which Node i does not have any frames, it is expressed as

$$b_{i,0} = 1 - Q_i \qquad (33)$$

Besides, since the sum of the steady-state probability that Node i has l frames is one, we obtain

$$\sum_{l=0}^{\infty} b_{i,l} = 1 \qquad (34)$$

By combining equations (32)–(34), we have

$$b_{i,l} = Q_i^l - Q_i^{l+1} \qquad (35)$$

Using the steady-state probability that the Node i has l frames from the above, the queueing delay of Node i is

$$D_{Q_i} = \sum_{l=1}^{L} \left[\frac{D_{M_i}}{2} + (l-1)D_{M_i}\right] b_{i,l} \qquad (36)$$

From equations (33) and (36), the total transmission delay at Node i is calculated as

$$D_i = D_{M_i} + D_{Q_i} \qquad (37)$$

From equation (37), we can obtain the end-to-end delay in the H-hop string network

$$D = \sum_{i=0}^{H-1} D_i \qquad (38)$$

From the above analysis, when the offered load is given, we can obtain the end-to-end throughput and delay by fixing $4H$ unknown parameters including $X_i, \tau_i, \gamma_i, Y_i$.

Evaluation results

This section presents the validation of the proposed analytical models. We compare the analytical results to simulation ones, as well as evaluate the network performance. We use the simulator, which has been developed in our laboratory. The simulator efficiently describes the operations of IEEE 802.11 wireless nodes. Moreover, the validity of our simulator is carefully discussed in Ikuma et al.[24] In our evaluation, the system parameters have been associated with the IEEE 802.11a standard. Table 1 gives the values of typical investigated parameters. We investigate the throughput and delay performance with the variations of η and the distance ED.

Throughput performance evaluation

Figure 4 shows comparison between the analytical and simulation results of the end-to-end throughput with different values of η (i.e. 2 and 5). In the figure, the throughput is investigated following the variation of offered load. With each value of η, we evaluate four different networks. From Figure 4(a), we can see that in the case of $\eta = 2$, the analytical predictions (in lines) well match with the simulation results (in plots). These results show that the proposed model covers the previous one in Sanada et al.,[19] which considers only the simple carrier-sensing range with $\eta = 2$. The comparison in Figure 4(b) is for the case of $\eta = 5$ with four networks (i.e. eight-hop, 12-hop, 17-hop, and 23-hop). The results in the figure again indicate that the analytical results agree with the simulation ones quantitatively, and that also confirm the applicability of proposed model in the condition where many nodes are within the carrier-sensing range. In other words, we have successfully applied the analysis with a wide range of η (other than only 2). From both figures, it can be seen that the proposed model can express the throughput values not only in the non-saturation condition but also the saturation one, and that shows the effectiveness of the proposed models under any conditions of offered loads.

Figure 5 shows the comparison of end-to-end throughput when the ED is fixed while the value of η is

Table 1. System parameters.

Payload	200 byte
Carrier-sensing range	150 m
Data rate ($\eta = 1$)	6 Mbps
Data rate ($\eta = 2, 3$)	18 Mbps
Data rate ($\eta = 4$)	36 Mbps
Data rate ($\eta = 5$)	54 Mbps
ACK bit rate ($\eta = 1$)	6 Mbps
ACK bit rate ($\eta = 2, 3$)	12 Mbps
ACK bit rate ($\eta = 4, 5$)	24 Mbps
SIFS	16 μs
DIFS	34 μs
Slot time (σ)	9 μs
CW_{min}	15
CW_{max}	1023
Retransmission limit (L)	7

ACK: ACKnowledgement; SIFS: short inter-frame space; DIFS: distributed inter-frame space.

varied from 1 to 5. We investigate two different scenarios with 350 m and 1200 m ED. Figure 5(a) and (b) shows the throughput results as a function of offered load different η for the case of $ED = 350\,\text{m}$ and $ED = 1200\,\text{m}$, respectively. From the both figures, we can observe that in case of $\eta = 2$, the largest end-to-end throughput (for the five-hop and 16-hop network) has been achieved in the evaluation. The reason is with $\eta = 2$, we got the best balance of transmission speed and transmission distance. Moreover, in all cases, we always see the agreements between the simulation and analytical results.

Delay performance evaluation

Similar to the previous evaluation, this section investigates the network performance when the offered load varies, but focusing on the end-to-end delay. Figure 6 shows the comparison of end-to-end delay values, which are collected from the simulation and analytical results. Wherein, Figure 6(a) and (b) shows the results for fixed-hop networks with $\eta = 2$ and $\eta = 5$, respectively. In the former figure, the hop number belongs to the set $\{1, 2, 4, 6, 10\}$ (hops), meanwhile the latter one has the set of $\{1, 5, 8, 12, 23\}$ (hops). From all figures in Figure 6, we can observe that the delay increases significantly as the hop number increases. The networks with a smaller number of hops tend to reach the high delay values sooner at the same condition of offered load. This is because network nodes close to the source node are a bottleneck where a large delay occurs compared with other network nodes. However, we can always see the good agreement means that the proposed model can express the end-to-end delay correctly in different conditions of η.

Figure 7 shows the end-to-end delay with different EDs, at each of which five fixed values of η are
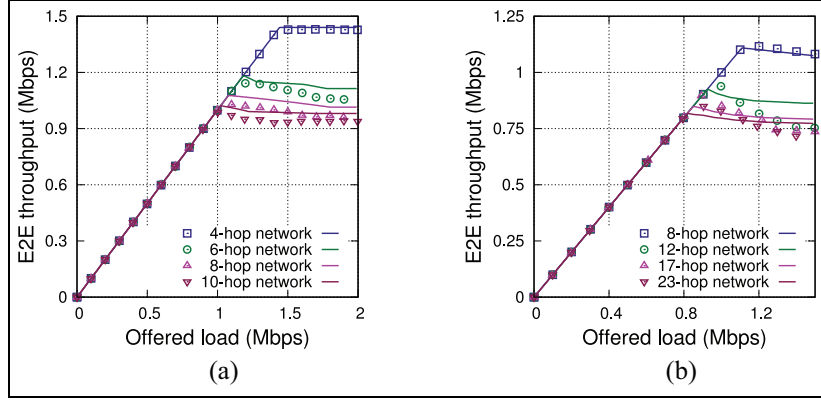
Figure 4. Comparing end-to-end (E2E) throughput between analytical model (lines) and simulation (plots) with different η: (a) $\eta = 2$ and (b) $\eta = 5$.
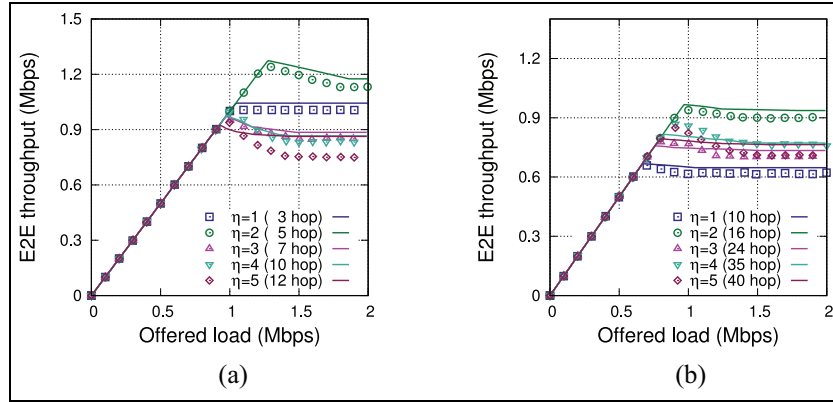

Figure 5. Comparing E2E throughput between analytical model (lines) and simulation (plots) in different *ED* scenarios: (a) end-to-end distance $ED = 350$ m and (b) end-to-end distance $ED = 1200$ m.
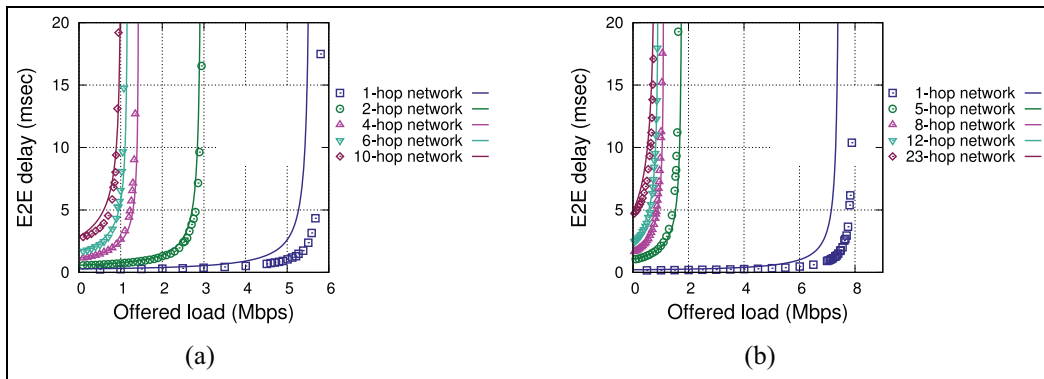

Figure 6. Comparing E2E delay between analytical model (lines) and simulation (plots) with different η: (a) $\eta = 2$ and (b) $\eta = 5$.

investigated. The results with $ED = 350$ m and $ED = 1200$ m are reported in Figure 7(a) and (b), respectively. In the figures, the analytical predictions again well match with the simulation results. Especially, we can observe the matched saturation points (i.e. between the saturated and unsaturated

conditions of the networks). In the unsaturated condition, it is seen when the η increases, the end-to-end delay also increases under the identical end-to-end distance when η is large, and that is because the number of hops dramatically increases with an increase in η.
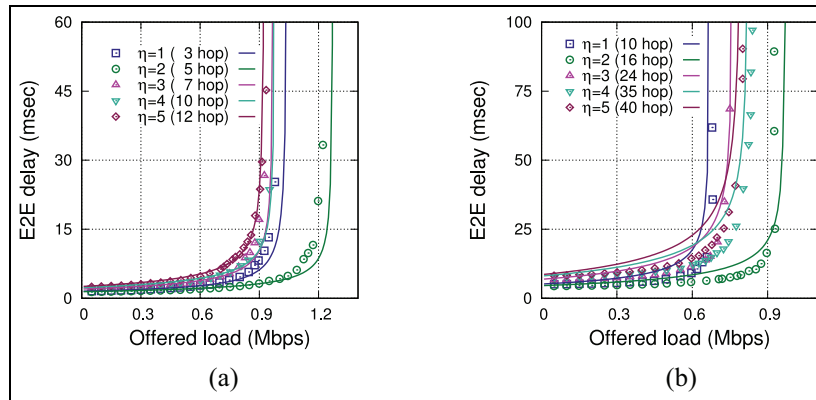
Figure 7. Comparing E2E delay between analytical model (lines) and simulation (plots) in different *ED* scenarios: (a) end-to-end distance *ED* = 350 m and (b) end-to-end distance *ED* = 1200 m.

Conclusion

In this work, we have proposed the new theoretical models for the IEEE 802.11 string-topology multi-hop networks' performance, including the end-to-end throughputs and delays. The models newly take into account the data rate by introducing the parameter η, which is the ratio of the carrier-sensing distance to the transmission one. By doing so, the applicability of models has been extended to a wide range of data rate values. Another novelty is that the modes consider the duplication time of frame transmissions, which are caused by the simultaneous transmission, especially in high-rate conditions. The analytical results in various topologies have been confirmedly matched with the simulation results to affirm the validity of the proposed models.

Declaration of conflicting interests

The author(s) declared no potential conflicts of interest with respect to the research, authorship, and/or publication of this article.

ORCID iD

Takeshi Kanematsu   https://orcid.org/0000-0001-9688-7782

Kien Nguyen   https://orcid.org/0000-0003-0400-3084

References

1. Nayak P and Vathasavai B. Energy efficient clustering algorithm for multi-hop wireless sensor network using type-2 fuzzy logic. *IEEE Sensor J* 2017; 17(14): 4492–4499.
2. Nguyen PL, Nguyen K, Vu H, et al. TELPAC: a time and energy efficient protocol for locating and patching coverage holes in WSNs. *J Netw Comput Appl* 2019; 147: 102439.
3. Nguyen K, Meis U and Ji Y. MAC2: a multi-hop adaptive MAC protocol with packet concatenation for wireless sensor networks. *IEICE Trans Inf Syst* 2012; E95.D(2): 480–489.
4. Chen G, Tang J and Coon JP. Optimal routing for multi-hop social-based D2D communications in the Internet of Things. *IEEE Internet Things J* 2018; 5(3): 1880–1889.
5. Hasan MZ, Al-Turjman F and Al-Rizzo H. Analysis of cross-layer design of quality-of-service forward geographic wireless sensor network routing strategies in green Internet of Things. *IEEE Access* 2018; 6: 20371–20389.
6. Chen G, Coon JP, Mondal A, et al. Performance analysis for multihop full-duplex IoT networks subject to Poisson distributed interferers. *IEEE Internet Things J* 2019; 6(2): 3467–3479.
7. Bellalta B, Belyaev E, Jonsson M, et al. Performance evaluation of IEEE 802.11p-enabled vehicular video surveillance system. *IEEE Commun Lett* 2014; 18(4): 708–711.
8. Alasmary W and Zhuang W. Mobility impact in IEEE 802.11p infrastructureless vehicular networks. *Ad Hoc Netw* 2012; 10(2): 222–230.
9. Mostafa A, Vegni AM and Agrawal DP. A probabilistic routing by using multi-hop retransmission forecast with packet collision-aware constraints in vehicular networks. *Ad Hoc Netw* 2014; 14(12): 118–129.
10. Chung NP and Liew SC. Throughput analysis of IEEE 802.11 multi-hop ad hoc networks. *IEEE/ACM Trans Netw* 2007; 15: 309–322.

11. Gao Y, Chiu D and Lui JCS. Determining the end-to-end throughput capacity in multi-hop networks: methodology and applications. In: *Proceedings of the ACM SIGMETRICS*, Saint-Malo, June 2006, pp.39–50. New York: ACM.

12. Inaba M, Tsuchiya Y, Sekiya H, et al. Analysis and experiments of maximum throughput in wireless multi-hop networks for VoIP application. *IEICE Trans Commun* 2009; E92-B(11): 3422–3431.

13. Sugimoto T, Komuro N, Sekiya H, et al. Maximum throughput analysis for RTS/CTS-used IEEE 802.11 DCF in wireless multi-hop networks. In: *Proceedings of the ICCCE*, Kuala Lumpur, Malaysia, 11–12 May 2010, pp.1–6. New York: IEEE.

14. Zhao H, Wang S, Xi Y, et al. Modeling intra-flow contention problem in IEEE 802.11 wireless multi-hop networks. *IEEE Commun Lett* 2010; 14(1): 18–20.

15. Sekiya H, Tsuchiya Y, Komuro N, et al. Analytical expression of maximum throughput for long-frame communications in one-way string wireless multihop networks. *Wireless Pers Commun* 2011; 60(1): 29–41.

16. Sanada K, Sekiya H, Komuro N, et al. Backoff-stage synchronization in three-hop string-topology wireless networks with hidden nodes. *Nonlinear Theory Appl IEICE* 2012; 3(2): 200–214.

17. Qinjuan Z, Muqing W, Jingrong W, et al. Bandwidth mapping model for IEEE 802.11 DCF in unsaturated condition. *IET Commun* 2012; 6(13): 2007–2015.

18. Shimoyamada Y, Sanada K, Komuro N, et al. End-to-end throughput analysis for IEEE 802.11e EDCA string-topology wireless multi-hop networks. *Nonlinear Theory Appl IEICE* 2015; E6-N(3): 410–432.

19. Sanada K, Komuro N, Li Z, et al. Generalized analytical expressions for end-to-end throughput of IEEE 802.11 string-topology multi-hop networks. *Ad Hoc Netw* 2018; 7(1): 135–148.

20. Sanada K, Shi J, Komuro N, et al. End-to-end delay analysis for IEEE 802.11 string-topology multi-hop networks. *IEICE Trans Commun* 2015; E98-B(7): 1284–1293.

21. Kanematsu T, Yoshida Y, Li Z, et al. Analytical evaluation of a WLAN with dense network nodes considering capture effect. *IEICE Trans Commun* 2020; E103-B(7): 815–825.

22. Liu J, Aoki T, Li Z, et al. Throughput analysis of IEEE 802.11 WLANs with inter-network interference. *Appl Sci* 2020; 10: 2192.

23. Kanematsu T, Nguyen K and Sekiya H. Throughput analysis for IEEE 802.11 multi-hop networks considering transmission rate. In: *Proceedings of the IEEE 89th vehicular technology conference*, Kuala Lumpur, Malaysia, 28 April–1 May 2019. New York: IEEE.

24. Ikuma S, Li Z, Pei T, et al. Rigorous analytical model of saturated throughput for the IEEE 802.11p EDCA. *IEICE Trans Commun* 2019; E102-B(4): 669–707.